Large reversible magnetocaloric effect in Tb_3Co compound

B. Li,[a] J. Du, W. J. Ren, W. J. Hu, Q. Zhang, D. Li, and Z. D. Zhang
Shenyang National Laboratory for Materials Science, Institute of Metal Research, and International Centre for Materials Physics, Chinese Academy of Sciences, 72 Wenhua Road, Shenyang 110016, People's Republic of China

(Received 25 March 2008; accepted 11 May 2008; published online 18 June 2008)

A large reversible magnetocaloric effect has been observed in Tb_3Co compound. Under a magnetic field change of 5 T, the maximum value of magnetic entropy change ΔS_M is -18 J kg^{-1} K^{-1} at 84 K and the relative cooling power is 738 J kg^{-1} with no hysteresis loss. In particular, the large reversible $\Delta S_M^{\max}$, -8.5 J kg^{-1} K^{-1}, is achieved for a low magnetic field change of 2 T. The magnetic anisotropy and the texture of the material greatly affect ΔS_M. The large reversible magnetocaloric effect (both the large ΔS_M and the high relative cooling power) indicates that Tb_3Co could be a promising candidate for magnetic refrigeration. © *2008 American Institute of Physics*.
[DOI: 10.1063/1.2939220]

The magnetic refrigeration based on magnetocaloric effect (MCE) has recently become a promising alternative of competitiveness to gas compression refrigeration technology widely in service, because of its energy-efficient and environment-friendly behavior.[1–12] However, MCE has been applied in magnetic refrigeration devices just in low temperature range ($T<20$ K) by using the paramagnetic salt $Gd_3Ga_5O_{12}$.[13] Accordingly, it is necessary to go on exploring advanced magnetic refrigerant materials with a large magnitude of isothermal magnetic entropy change ΔS_M and/or adiabatic temperature change ΔT_{ad} for the purpose of magnetic refrigerant application from 20 K up to room temperature.[6] Typically, the giant MCE observed in different systems is closely related to a field-induced first-order phase transition.[5] Unfortunately, the first-order phase transition usually leads to considerable thermal and magnetic hysteresis that will consume the relative cooling power (RCP) of magnetic refrigerant materials.[7–12,14–17] The disadvantages mentioned confine their application. It should be realistic to search advanced magnetic refrigerant materials with a large reversible ΔS_M based on the second-order phase transitions. In particular, realizing a large reversible ΔS_M at a comparatively low field is very important for application. In this letter, we report the large reversible MCE of Tb_3Co, which results from a second-order phase transition. More important, the large reversible $\Delta S_M^{\max}$, -8.5 J kg^{-1} K^{-1}, is achieved for a low magnetic field change of 2 T. It is also observed that the magnetic anisotropy and the texture of the material greatly affect the MCE performance.

Polycrystalline Tb_3Co compound was prepared by melting constituent elements with a purity of 99.9% under argon atmosphere. The ingot was annealed in an evacuated and sealed silica tube at 600 °C for 4 days for homogeneousness. The x-ray diffraction pattern confirms the single-phase nature of the compound, crystallizing in the orthorhombic Fe_3C-type structure (space group *Pnma*).[18] The lattice parameters *a*, *b*, and *c*, were determined to be 7.00, 9.41, and 6.28 Å, respectively, by using Rietveld refinement method, which are consistent with the previous report.[18] Magnetic properties were measured by using a superconducting quantum inference device magnetometer (Quantum Design) from 50 K to the paramagnetic (PM) state of the compound and at applied magnetic fields up to 7 T.

The 3*d* band in Tb_3Co is completely filled by 6*s* and 5*d* electrons from rare earth atoms, which results in the magnetic ordering essentially dominated by Ruderman–Kittel–Kasuya–Yosida indirect interactions between the rare earth ions, via the conduction electrons.[19] Tb_3Co processes a complex magnetic structure, in which there is a strong ferromagnetic (FM) component parallel to *c* axis and antiferromagnetic (AF) one along *a* and *b* axes at low temperatures.[20] Such complex structure will bring interesting physical properties.

Temperature dependences of zero-field-cooling (ZFC) and field-cooling (FC) magnetization at a magnetic field of 0.005 T are represented in Fig. 1. According to neutron diffraction investigation by Baranov *et al.*,[20] Tb_3Co undergoes two successive transitions at temperatures $T_t=72$ K (FM/AF) and $T_N=82$ K (AF/PM), corresponding to the maximum slopes in the *M*-*T* curve. The neutron diffraction investigation suggested that the incommensurate FM state, at T_t for a first-order magnetic phase transition, develops to a modulated AF state that exists below T_N.[20] On the other hand, reversible behavior above 50 K in ZFC and FC curves at a

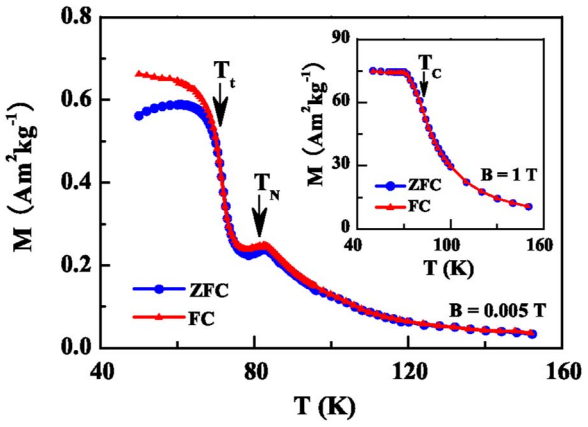

FIG. 1. (Color online) Temperature dependences of ZFC and FC magnetization at a magnetic field of 0.005 T of Tb_3Co. The inset is for ZFC-FC curves at 1 T.

[a]Electronic mail: libing@imr.ac.cn.

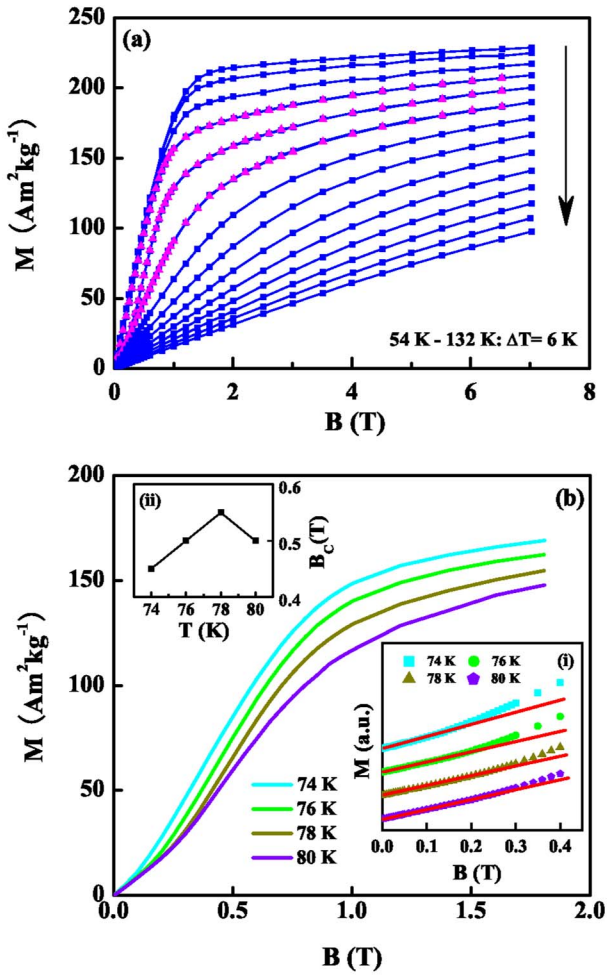

FIG. 2. (Color online) (a). Magnetic isothermals of Tb_3Co in the temperature range of 54–132 K measured on field increase (solid squares) and field decrease (solid triangles), with temperature step of 6 K. (b) Magnetic isothermals in the low magnetic field region at 74, 76, 78, and 80 K, respectively. The inset (i) illustrates the deviation from the linear magnetization-field relationship, while the inset (ii) gives the temperature dependence of $B_c(T)$.

magnetic field of 1 T (see the inset of Fig. 1) indicates that Tb_3Co experiences a second-order FM to PM phase transition at T_c=82 K. Arrott plots below also confirm its second-order nature. It can be deduced from Fig. 1 and its inset that a small magnetic field, less than 1 T, can induce a metamagnetic transition from AF to FM state.

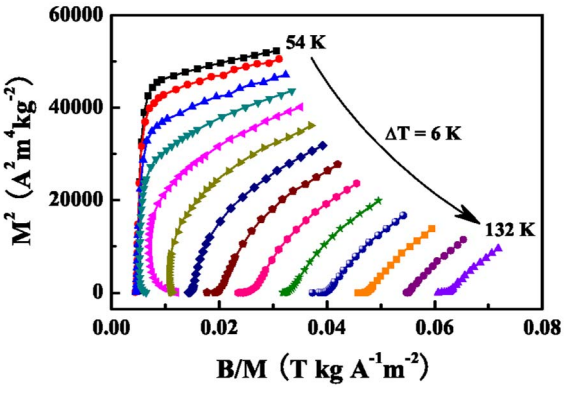

FIG. 3. (Color online) The Arrott plots of Tb_3Co from 54 to 132 K with the temperature step of 6 K.

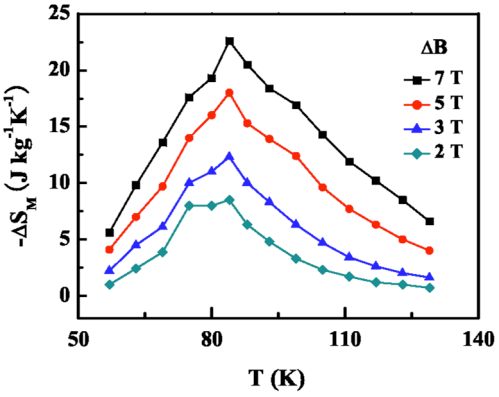

FIG. 4. (Color online) Temperature dependence of the magnetic entropy change ΔS_M of Tb_3Co at the magnetic field changes ΔB of 2, 3, 5, and 7 T.

A set of selected magnetic isothermals measured on increasing (solid squares) and decreasing field (solid triangles) are shown in Fig. 2(a) for Tb_3Co, with temperature step of 6 K from 54–132 K. It can be seen from Fig. 2(a) that there is very little magnetic hysteresis around the transition temperature. The metamagnetic transition as well as a significant magnetoresistance effect has been investigated on Tb_3Co single crystals.[21] Figure 2(b) displays in detail the metamagnetic AF to FM transitions in the low magnetic field region at 74, 76, 78, and 80 K, respectively. As shown in the inset (i) of Fig. 2(b), the magnetization remains a linear relationship with the magnetic field at low magnetic field region, suggesting the existence of AF state. The AF state starts to develop to FM state, when magnetization curves deviate from such linear relationship. One could define a critical magnetic field $B_c(T)$ for the metamagnetic transition, corresponding to the maximum value of dM/dB. Eventually, the AF state will completely transform into the FM one when the magnetic field approaches about 2 T. The change in $B_c(T)$ with temperature is represented in the inset (ii) of Fig. 2(b), which agrees with the previous report.[21] The Arrott plots with the temperature step of 6 K from 54 to 132 K are shown in Fig. 3. The negative slopes at the low magnetic field region at 72 and 78 K indicate the first-order nature of the metamagnetic phase transition from AF to FM state. On the other hand,

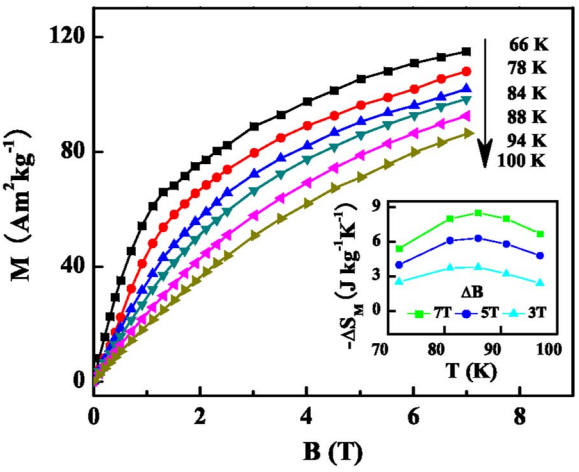

FIG. 5. (Color online) Magnetic isothermals of the fixed powders of Tb_3Co. The inset is for temperature dependence of the magnetic entropy change ΔS_M of the fixed powders Tb_3Co at the magnetic field changes ΔB of 3, 5, and 7 T.

TABLE I. Comparison of the representative refrigerant materials based on the second-order transition with working span of temperature around 80 K.

Material	$-\Delta S_M^{\max}$ (5 T) (J kg^{-1} K^{-1})	RCP (5 T) (J kg^{-1})	$-\Delta S_M^{\max}$ (2 T) (J kg^{-1} K^{-1})	RCP (2 T) (J kg^{-1})	Transition temperature (K)	Reference
TbCoAl	10.5	~420	5.3	~212	70	25
$CdCr_2S_4$	7.04	~360	3.92	~130	87	22
Tb_3Co	18	~738	8.5	~306	82	This work

Arrott plots above T_c in which there is neither the inflection point nor the negative slopes suggest the occurrence of a second-order phase transition,[22] which agrees with the inset of Fig. 1.

A large MCE is expected around T_c where the magnetization rapidly changes with varying temperature. The isothermal magnetic entropy change $\Delta S_M(T,B)$ is given by integrating Maxwell relation,

$$\Delta S_M(T,B) = \int_0^B \left(\frac{\partial M}{\partial T}\right)_B dB. \quad (1)$$

The temperature dependences of $\Delta S_M(T,B)$ under different magnetic field changes calculated by using formula (1) are displayed in Fig. 4. $\Delta S_M^{\max}$ are −8.5, −12.3, −18, and −22.6 J kg^{-1} K^{-1}, respectively, for the magnetic field changes of 2, 3, 5, and 7 T. The large $\Delta S_M^{\max}$, −8.5 J kg^{-1} K^{-1}, achieved for a low magnetic field change of 2 T, is beneficial to application. The peaks of ΔS_M at 84 K just correspond to the FM to PM phase transition. The magnetic anisotropy has been reported to affect the magnetic entropy change and thus the fixed powder sample was investigated.[23] The selected magnetic isothermals of the fixed powder sample of Tb_3Co are displayed in Fig. 5. The inset of Fig. 5 represents the temperature dependence of the magnetic entropy change calculated by using formula (1). It is obvious that $\Delta S_M^{\max}$ of the fixed powders is less than half of the bulk counterpart. This is because the magnetization of the fixed powders is randomly oriented, while that of the bulk with the texture has the preferential orientation.

The RCP is a measure of how much heat can be transferred between the cold and hot sinks in one ideal refrigerant cycle,[5] which is of practical significance. The RCP value can be calculated by using a method for conventional refrigerant materials, as follows,[24]

$$\mathrm{RCP} = -\Delta S_M^{\max} \delta T_{\mathrm{FWHM}}, \quad (2)$$

where, δT_{FWHM} is the full width at half maximum of the ΔS_M-T curve. For Tb_3Co, the ΔS_M spans in a wide temperature range and the δT_{FWHM} approaches to ~36 and ~41 K for the magnetic field changes of 2 and 5 T, respectively. Consequently, the RCP values for Tb_3Co are 306 and 738 J kg^{-1}, respectively. For clarity, we summarize in Table I the main parameters of the representative refrigerant materials around 80 K that undergo the second-order phase transitions.[22,25] As shown in Table I, Tb_3Co is an excellent candidate for magnetic refrigeration owing to its high reversible RCP.

In conclusion, the large reversible MCE with $\Delta S_M^{\max}$ of −18 J kg^{-1} K^{-1} at 84 K for a magnetic field change of 5 T is achieved in Tb_3Co with a reversible RCP value of 738 J kg^{-1}. In particular, the large reversible $\Delta S_M^{\max}$ (8.5 J kg^{-1} K^{-1}) and RCP (306 J kg^{-1}) are obtained for a low magnetic field change of 2 T. The magnetic anisotropy and the texture of the material greatly affect the MCE performance. The large ΔS_M with the high reversible RCP indicates that Tb_3Co could be a promising candidate for magnetic refrigeration.

This work has been supported by the National Natural Science Foundation of China under Grant No. 50331030.

[1] E. Warburg, Ann. Phys. **13**, 141 (1881).
[2] C. B. Zimm, A. Jastrab, A. Sternberg, V. K. Pecharsky, K. A. Gschneidner, Jr., M. Osborne, and I. Anderson, Adv. Cryog. Eng. **43**, 1759 (1998).
[3] J. Glanz, Science **279**, 2045 (1998).
[4] V. K. Pecharsky and K. A. Gschneidner, Jr., J. Magn. Magn. Mater. **200**, 44 (1999).
[5] K. A. Gschneidner, Jr., V. K. Pecharsky, and A. O. Tsokol, Rep. Prog. Phys. **68**, 1479 (2005).
[6] E. Brück, O. Tegus, D. T. C. Thanh, and K. H. J. Buschow, J. Magn. Magn. Mater. **310**, 2793 (2007).
[7] V. K. Pecharsky and K. A. Gschneidner, Jr., Phys. Rev. Lett. **78**, 4494 (1997).
[8] A. de Campos, D. L. Rocco, A. M. G. Carvalho, L. Caron, A. A. Coelho, S. Gama, L. M. da Silva, F. C. G. Gandra, A. O. dos Santos, L. P. Cardoso, P. J. von Ranke, and N. A. de Oliveira, Nat. Mater. **5**, 802 (2006).
[9] N. K. Sun, W. B. Cui, D. Li, D. Y. Geng, F. Yang, and Z. D. Zhang, Appl. Phys. Lett. **92**, 072504 (2008).
[10] T. Krenke, E. Duman, M. Acet, E. F. Wassermann, X. Moya, L. Manosa, and A. Planes, Nat. Mater. **4**, 450 (2005).
[11] O. Tegus, E. Brück, K. H. J. Buschow, and F. R. de Boer, Nature (London) **415**, 150 (2002).
[12] F. X. Hu, B. G. Shen, J. R. Sun, Z. H. Cheng, G. H. Rao, and X. X. Zhang, Appl. Phys. Lett. **78**, 3675 (2001).
[13] J. A. Barclay and W. A. Steyert, Cryogenics **22**, 73 (1982).
[14] O. Tegus, E. Brück, L. Zhang, W. Dagula, K. H. J. Buschow, and F. R. de Boer, Physica B **319**, 174 (2002).
[15] J. Du, W. B. Cui, Q. Zhang, S. Ma, D. K. Xiong, and Z. D. Zhang, Appl. Phys. Lett. **90**, 042510 (2007).
[16] N. K. Sun, S. Ma, Q. Zhang, J. Du, and Z. D. Zhang, Appl. Phys. Lett. **91**, 112503 (2007).
[17] V. Provenzano, A. J. Shapiro, and R. D. Shull, Nature (London) **429**, 853 (2004).
[18] E. Pathe and J. M. Moreau, J. Less-Common Met. **53**, 1 (1977).
[19] D. Gignoux, J. C. Gomez-Sal, and D. Paccard, Solid State Commun. **44**, 695 (1982).
[20] N. V. Baranov, A. F. Gubkin, A. P. Vokhmyanin, A. N. Pirogov, A. Podlesnyak, L. Keller, N. V. Mushnikov, and M. I. Bartashevich, J. Phys.: Condens. Matter **19**, 326213 (2007).
[21] N. V. Baranov, P. E. Markin, H. Nakotte, and A. Lacerda, J. Magn. Magn. Mater. **177-181**, 1133 (1998).
[22] L. Q. Yan, J. Shen, Y. X. Li, F. W. Wang, Z. W. Jiang, F. X. Hu, J. R. Sun, and B. G. Shen, Appl. Phys. Lett. **90**, 262502 (2007).
[23] X. X. Zhang, H. L. Wei, Z. Q. Zhang, and L. Y. Zhang, Phys. Rev. Lett. **87**, 157203 (2001).
[24] K. A. Gschneidner, Jr., and V. K. Pecharsky, Annu. Rev. Mater. Sci. **30**, 387 (2000).
[25] X. X. Zhang, F. W. Wang, and G. H. Wen, J. Phys.: Condens. Matter **13**, L747 (2001).